

VITRIFIED BOTTOM ASH SLAG FROM MUNICIPAL SOLID WASTE INCINERATORS - PHASE RELATIONS OF CaO-SiO₂-Na₂O OXIDE SYSTEM

Zhan Zhang, Yanping Xiao, Yongxiang Yang, Rob Boom & Jack Voncken

Delft University of Technology, The Netherlands

ABSTRACT

Vitrification is considered to be an attractive technology for bottom ash treatment because it destroys the hazardous organics, contributes to immobilization of the heavy metals, and additionally it reduces drastically the volume. The main components of the vitrified bottom ash slag are SiO₂, CaO, Al₂O₃, Fe₂O₃, Na₂O and MgO, and the compositions have direct effect on the glass formation during vitrification, and further on the physical and mechanical properties of the slag.

To provide essential data for the utilization of bottom ash as vitrified slag, the phase relations and thermodynamic properties of the oxide system need to be systematically investigated. In the present study, the liquidus temperature of the typical vitrified bottom ash slag was determined by using Differential Scanning Calorimetry (DSC) measurement. High temperature equilibrium experiments were conducted to investigate the phase relations of the vitrified slag and sub-oxide system CaO-SiO₂-Na₂O by means of Scanning Electron Microscopy (SEM), Electron Microprobe Analysis (EMPA) and X-ray Diffraction (XRD). The results show that the melting temperature of the vitrified bottom ash is around 1120°C. In the CaO-SiO₂-Na₂O system with less than 50 mol% SiO₂, the liquidus temperature increases with increasing amounts of Na₂O along the tie-line of Na₂O-Ca₃Si₂O₇. The compound of Na₂Ca₃Si₂O₈ is identified in the oxide system.

INTRODUCTION

Incineration is an effective technology to convert waste to energy and to significantly reduce the solid waste volume (by up to 90%). Multiple solid waste incinerators produce a large amount of solid residues in which bottom ash accounts for about 85% by weight [2]. Bottom ash utilization in the Netherlands is about 100%, mainly for construction of road and buildings. Leaching of heavy metals is a potential problem for recycling and utilization of bottom ash. Various methods were tested to process and immobilize the bottom ash. The most important ways are ageing, clinker production, natural weathering, carbonation, mixing with cement or carbon rich binder from oil refining, addition to clay-based bricks or asphalt, and vitrification [7]. Vitrification is considered to be an attractive approach for bottom ash treatment because it can completely destroy the toxic organics, it contributes to immobilization of the heavy metals and reduces drastically the waste volume. Therefore vitrification is expected to be widely used to treat bottom ash in the future.

MSW incineration bottom ash has a complex chemical composition that can be transformed into glassy slag by vitrification. Previous research indicates that the primary oxide components of the vitrified bottom ash slag are SiO_2 , CaO , Al_2O_3 , Fe_2O_3 , Na_2O and MgO [10]. In total they account for more than 90% of the bottom ash by weight. These compositions have direct effect on the glass formation during vitrification, and further on the mineralogical and mechanical properties of the slag. A number of studies have been carried out on use of bottom ash in glass-ceramic products. In order to provide essential fundamental knowledge for recycling and utilization of the bottom ash, the above mentioned multi-oxide system should be investigated systematically. So far very little systematic research work has been reported.

The ternary oxide system $\text{Na}_2\text{O-CaO-SiO}_2$, one subsystem of the complex $\text{SiO}_2\text{-CaO-Al}_2\text{O}_3\text{-Fe}_2\text{O}_3\text{-Na}_2\text{O-MgO}$ system, is of considerable importance to the glass industry. Morey & Bowen carried out the first study on the phase equilibrium relations in this ternary system [6]. In this study they found ten primary phases, including SiO_2 (cristobalite, tridymite, quartz), $\alpha\text{-CaSiO}_3$, $\beta\text{-CaSiO}_3$, Na_2SiO_3 , $\text{Na}_2\text{Si}_2\text{O}_5$, and three ternary compounds $\text{Na}_2\text{Ca}_2\text{Si}_3\text{O}_9$, $\text{Na}_4\text{CaS}_3\text{O}_9$ and $\text{Na}_2\text{Ca}_3\text{Si}_6\text{O}_{16}$. The latter two phases have incongruent melting points. Morey [5] investigated the phase equilibrium in the low-lime and high-silica regions in detail. In 1965, Williamson and Glasser discovered an incongruent point of sodium silicate $\text{Na}_6\text{Si}_8\text{O}_{19}$ [9], which was not encountered by Morey and Bowen [6]. The high-silica region of the soda-lime-silica ternary system has attracted a great attention due to its importance to glass technology. However, little investigation has been undertaken to extend the phase equilibrium relations into the regions with less than 50 mol% silica except the work presented by Segnit [8]. In Segnit's research nine ternary invariant points including $\text{Ca}_2\text{SiO}_4\text{-Na}_2\text{CaSiO}_4\text{-CaSiO}_3$ were determined.

The objectives of the present study are to investigate the thermal behaviour of vitrified bottom ash slag. With the particular interest for the bottom ash application, the phase relations of ternary subsystem $\text{Na}_2\text{O-CaO-SiO}_2$ were investigated focusing more on the low Na_2O composition region. The properties of the vitrified slag were evaluated in comparison with the synthetic oxide slag. This research is also aimed to extend the knowledge of the phase equilibrium of this ternary system to the area of relative low silica.

EXPERIMENTAL

System Selections

Table 1 shows the typical composition of the vitrified bottom ash slag from AVR in Rozenburg of the Netherlands [10]. The vitrified bottom ash slag from previous research [10] was finely ground in an agate mortar for DSC measurements. The synthesized slag was prepared according to the normalized composition presented in Table 1.

Table 1: Major compositions of typical vitrified bottom ash and synthetic slag

| | Oxide | Vitrified bottom ash slag, wt% synthetic slag, wt% |
|--------------------------------|-------|---|
| SiO ₂ | 52.10 | 55.02 |
| CaO | 16.20 | 17.11 |
| Al ₂ O ₃ | 12.20 | 12.88 |
| Fe ₂ O ₃ | 7.70 | 8.13 |
| Na ₂ O | 4.20 | 4.44 |
| MgO | 2.30 | 2.42 |
| TiO ₂ | 1.30 | - |
| K ₂ O | 1.10 | - |

Samples of the Na₂O-CaO-SiO₂ oxide mixtures with well defined compositions were prepared with the same methods. The compositions were selected to be in the Na₂SiO₃-CaSiO₃-SiO₂ region (C series) and the relatively lime rich region (A and B series) as illustrated in Figure 1. One test (D) located on the tie line of Ca₂SiO₃-Na₂CaSiO₄ was also investigated based on the results of series B. The compositions of the samples are listed in Table 2.

Table 2: Compositions of the samples in the Na₂O-CaO-SiO₂ system

| Sample | Composition (mol%) | | |
|----------------|----------------------|------|------------------|
| | Na ₂ O | CaO | SiO ₂ |
| A ₁ | 5.0 | 47.5 | 47.5 |
| A ₂ | 10.0 | 45.0 | 45.0 |
| A ₃ | 15.0 | 42.5 | 42.5 |
| B ₁ | 5.0 | 57.0 | 38.0 |
| B ₂ | 10.0 | 54.0 | 36.0 |
| B ₃ | 15.0 | 51.0 | 34.0 |
| C ₁ | 5.0 | 28.5 | 66.5 |
| C ₂ | 10.0 | 27.0 | 63.0 |
| C ₃ | 15.0 | 25.5 | 59.5 |
| D | 28.6 | 42.8 | 28.6 |

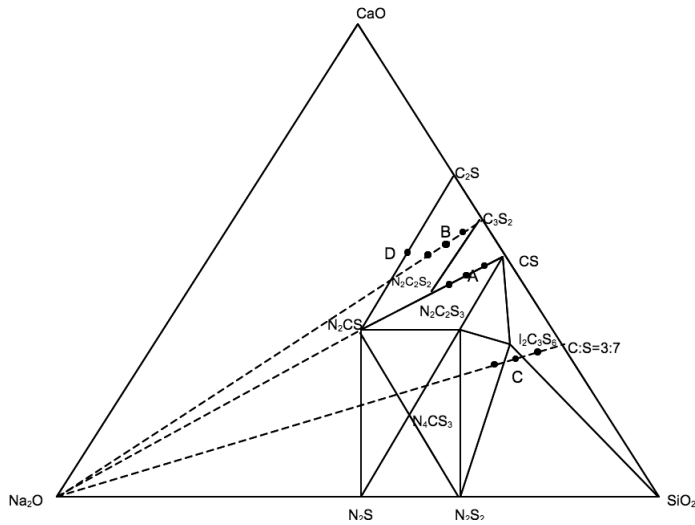


Figure 1: Compositions of the Na_2O - CaO - SiO_2 system (N for $\text{NaO}_{0.5}$, C for CaO and S for SiO_2)

Materials

Laboratory reagent grade powders of CaCO_3 , Al_2O_3 , SiO_2 , Fe_2O_3 , MgO , and Na_2CO_3 with purity level of 99.5% were used for slag synthesis. The required oxide powders were well mixed in a mixing mill and preheated at 1100°C for 4 hours in a chamber furnace to decompose CaCO_3 and Na_2CO_3 . This minimizes the heterogeneity of the mixture sample and promotes the phase transformation and melting of the mixture. The sintered mixture was again finely ground for DSC analysis.

Experimental Procedures

DSC-measurements were carried out with Netzsch STA409 simultaneous thermal analyzer using platinum crucibles under argon atmosphere with a flow of 50 ml/min. About 50 (± 0.5) mg sample was heated from room temperature to 1500°C at the rate of $10^\circ\text{C}/\text{min}$. The temperature was calibrated against the melting point of pure metals. An empty platinum crucible was employed as reference for thermal balance.

Equilibrium experiments were conducted in an electrical resistance tube furnace at the temperature determined from DSC measurement. About 20 (± 1)g sample was charged in a platinum crucible and placed in the constant temperature zone of the furnace. Nitrogen gas at a flow rate of 50 ml/min was used as protecting gas. The temperature of the sample was measured with a Pt-PtRh10 thermocouple which was calibrated against a standard thermocouple. The sample was heated at a rate of $10^\circ\text{C}/\text{min}$, and kept at the equilibrium temperature for a period of 4 to 24 hours. After the equilibrium, the sample was rapidly quenched under nitrogen atmosphere.

The equilibrated samples were embedded in epoxy resin and subsequently polished for microstructural investigation with Scanning Electron Microscopy (SEM) and Electron Microprobe Analysis (EMPA). In addition, the vitrification tendency and the crystalline phases present in the equilibrated sample were identified with X-ray Diffractometry (XRD).

RESULTS AND DISCUSSION

Thermal Behaviour of the Vitrified Bottom Ash Slag

The thermal behaviour of the vitrified bottom ash slag and the synthetic slag is shown in Figure 2 according to the DSC measurements. No obvious weight change was observed when the two samples were heated from 20°C to 1500°C. Few reaction peaks could be detected in the synthetic slag due to the pre-heat treatment at 1100°C for 4 hours (sintering) before the thermal behavior investigation. For the vitrified bottom ash slag, several reaction peaks can be identified from 800°C to 1100°C in the DSC curve possibly due to its complex chemical composition. The dramatic endothermic reactions starting at approximately 1100°C indicate the onset of the melting of the two slag samples. But it is clear that the melting point of the synthetic oxide slag (~1110°C) is about 10°C lower than the vitrified bottom ash slag (~1120°C). This result is in a good agreement with the investigation of Barbieri [1]. However, the glass transition temperature between 600°C and 700°C of the vitrified bottom ash slag as reported by Barbieri [1] is not identified in this study, because of the pre-vitrification of the original bottom ash sample. So far the exact nature of the reactions taking place in the vitrified slag is unknown, due to the complexity of the chemical system.

For the equilibrium experiments, the vitrified bottom ash slag and the synthetic slag were quenched under nitrogen atmosphere after keeping equilibrated at 1110°C for 24 hours in a tube furnace. Then the crystalline phases in the quenched samples were analyzed with XRD. In general, the XRD patterns recorded on the above samples show that there is not much difference between the vitrified slag and the synthetic slag. The result is shown in Figure 3. In both samples, $\text{CaMg}(\text{SiO}_3)_2$ and CaSiO_3 were determined to be the thermodynamically most favored phases. However, Al_2O_3 and MgO were found in the synthetic slag and MgO phase was also identified in the vitrified bottom ash slag. The results investigated by Ferraris and Salvo [3] show that $\text{CaMgSi}_2\text{O}_6$, Al_2O_3 and MgO are the primary phase present in bottom ash slag which is in agreement with the present results. Since the relative high SiO_2 concentration in the bottom ash slag, the dominant phase is in an amorphous state in the quenched sample.

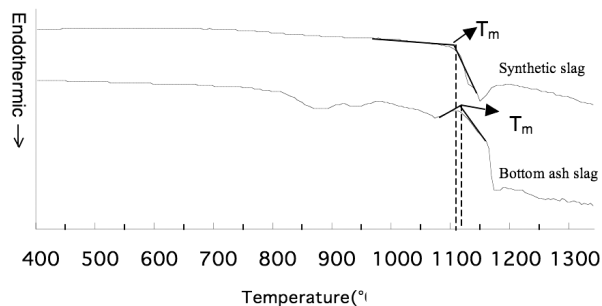


Figure 2: Thermal behaviour of the vitrified bottom ash slag and the synthetic slag

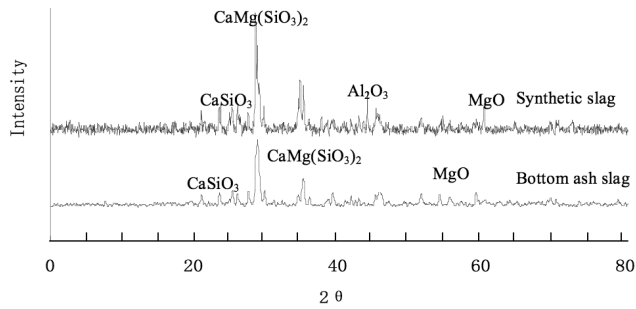


Figure 3: X-ray diffraction pattern of the vitrified bottom ash slag and synthetic slag at 1110°C

Phase Relations of the $\text{Na}_2\text{O}-\text{CaO}-\text{SiO}_2$ Oxide System

The compositions of the C series samples were selected in the $\text{Na}_2\text{SiO}_3-\text{CaSiO}_3-\text{SiO}_2$ region as shown in Figure 1. The results of the DSC measurements prove that the liquidus temperature decreases with increasing the sodium oxide content which agrees with that reported in the literature [8]. In the SiO_2 rich region several crystalline phases were identified in this work: SiO_2 as quartz and tridymite, the α -modification of $\text{Na}_2\text{Si}_2\text{O}_5$, $\text{Na}_6\text{Si}_8\text{O}_{19}$, and the ternary compounds $\text{Na}_2\text{Ca}_3\text{Si}_6\text{O}_{16}$. Compound $\text{Na}_2\text{CaSi}_5\text{O}_{12}$ identified by Shahid and Glasser [9] was not found in this work.

In the low SiO_2 concentration region Series A and B were investigated. The compositions of the A series samples as shown in Table 2 and Figure 1 lie in the region containing less than 50 mol% silica, close to the pseudo-binary system of $\text{CaSiO}_3-\text{Na}_2\text{SiO}_3$ which has also been examined by Moir and Glasser [4]. From the results of DSC analysis, the liquidus temperature in this series has the same tendency to the series C. According to the analysis of microstructure and crystalline phases, five primary phases, pseudowollastonite (α - CaSiO_3), dicalcium silicate (Ca_2SiO_4), $\text{Ca}_3\text{Si}_2\text{O}_7$, $\text{Na}_2\text{Ca}_2\text{Si}_3\text{O}_9$ and $\text{Na}_2\text{Ca}_2\text{Si}_2\text{O}_7$, were confirmed. Figure 4 shows the three crystalline phases of the sample containing least sodium oxide in series A, which was also identified clearly in the SEM micrograph: dark grey groundmass (labeled 1) with brighter needle (labeled 3) shaped crystals and more or less equidimensional crystals (labeled 2).

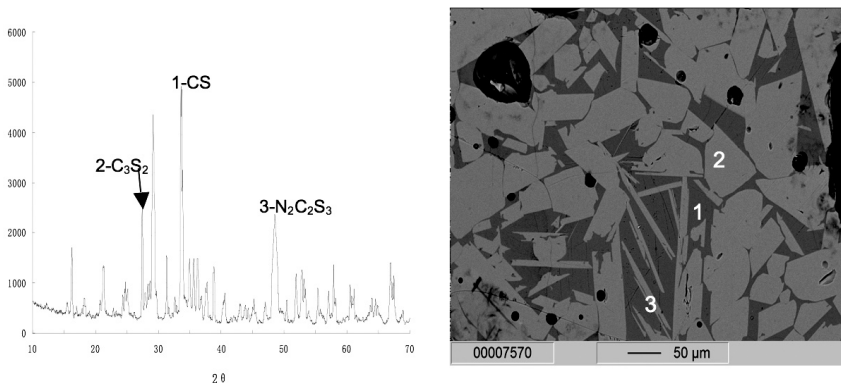


Figure 4: XRD and SEM analysis of sample in series A at 1270°C (N for $\text{NaO}_{0.5}$, C for CaO and S for SiO_2)

Compound $\text{Na}_2\text{Ca}_2\text{Si}_2\text{O}_7$ identified in series A has not been described in details in the literature. The melting point of this compound was investigated by Segnit [8]. A sample of the compound quenched from 1446°C is almost entirely glassy. The melting point of the pure compound will be close to 1450°C . Its primary phase field is bordered by those of $\alpha\text{-CaSiO}_3$, Ca_2SiO_4 , $\text{Ca}_3\text{Si}_2\text{O}_7$, $\text{Na}_2\text{Ca}_2\text{Si}_3\text{O}_9$ and $\text{Na}_2\text{CaSiO}_4$.

Series B compositions lie in the ternary invariant point ($\text{Ca}_2\text{SiO}_4\text{-Na}_2\text{CaSiO}_4\text{-CaSiO}_3$) area as shown in Figure 1. From DSC analysis, the melting temperature slightly increases with increasing Na_2O concentration. Based on the results obtained by XRD analysis on quenched samples, five different compounds can be identified, $\alpha\text{-CaSiO}_3$, $\text{Ca}_3\text{Si}_2\text{O}_7$, $\text{Na}_2\text{CaSiO}_4$, Ca_2SiO_4 and $\text{Na}_2\text{Ca}_3\text{Si}_2\text{O}_8$. The first three of these compounds have been described in literature [6]. The compound $\text{Na}_2\text{Ca}_3\text{Si}_2\text{O}_8$ identified in this study is located on the tie line between Ca_2SiO_4 and $\text{Na}_2\text{CaSiO}_4$. Segnit has investigated phase equilibrium relationships in this area. However, no description on this crystalline phase was recorded in his work. To confirm the formation of $\text{Na}_2\text{Ca}_3\text{Si}_2\text{O}_8$, the point D in the middle of Ca_2SiO_4 and $\text{Na}_2\text{CaSiO}_4$ as shown in Figure 1 was selected to investigate the equilibrium phases with the same procedure. The melting point of sample D is determined to be approximately 1330°C . The equilibrium test was performed at 1315°C , and the quenched sample was scanned with XRD. The result is shown in Figure 5. From the presence of the XRD patterns, the compound $\text{Na}_2\text{Ca}_3\text{Si}_2\text{O}_8$ can be confirmed, as well as the phases of $\text{Na}_2\text{CaSiO}_4$ and Ca_2SiO_4 . The thermodynamic property of the compound $\text{Na}_2\text{Ca}_3\text{Si}_2\text{O}_8$ is not found in the literature, and further research will be conducted for a systematic investigation.

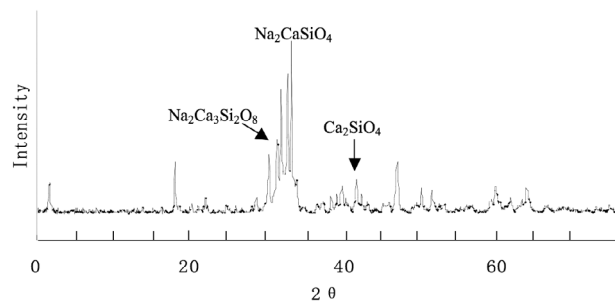


Figure 5: X-ray diffraction pattern of the sample D between $\text{Na}_2\text{CaSiO}_4$ and Ca_2SiO_4 at 1315°C

CONCLUSIONS

The results of the DSC measurements performed on the vitrified bottom ash slag and the synthetic slag show that the melting temperature of the synthetic slag is approximately 1110°C , and that of the vitrified bottom ash slag is about 1120°C (10 degrees higher than the synthetic slag). The XRD patterns recorded on the both types of the samples at 1110°C present no obvious differences. The two compounds $\text{CaMgSi}_2\text{O}_6$ and CaSiO_3 were found to be the thermodynamically most favored phases at 1100°C . Alumina phase was identified in the vitrified bottom ash slag but not in the synthetic slag. The results obtained from the experiments indicate that the properties of the synthetic slag is close to the vitrified slag from the industrial bottom ash.

For the ternary subsystem $\text{Na}_2\text{O-CaO-SiO}_2$, the liquidus temperature and crystalline phase relations in relative low Na_2O region were confirmed. Phase relations in relative low silica region were extended. In general, the liquidus temperature increases with increasing

amounts of Na_2O . The melting temperature of the middle point between $\text{Na}_2\text{CaSiO}_4$ and Ca_2SiO_4 was obtained as approximately 1330°C . The compound $\text{Na}_2\text{Ca}_3\text{Si}_2\text{O}_8$ located on the tie line between Ca_2SiO_4 and $\text{Na}_2\text{CaSiO}_4$ is identified as a new compound which is not reported in the literature. The thermodynamic properties of ternary subsystem $\text{Na}_2\text{O-CaO-SiO}_2$ will be utilized to further investigate the vitrified bottom ash in the future.

ACKNOWLEDGEMENTS

This research was carried out within the Project 06DP040 – Reducing Secondary Environmental Risk from Waste Incineration, supported by Royal Netherlands Academy of Arts and Science (KNAW). The authors thank Mr Guus van Schijndel for preparing samples and performing equilibrium testing together. The XRD analysis from the analytical group in Department of Materials Science and Engineering, Delft University of Technology is acknowledged.

REFERENCES

- Barbieri, L. & Corradi, A. (2000). Alkaline & Alkaline-Earth Silicate Glasses and Glass-Ceramics from Municipal & Industrial Wastes. *Journal of the European Ceramic Society*, 20, pp. 1637-1643. [1]
- Dykstra, E. J. & Eighmy, T. T. (1998). *Petrogenesis of Municipal Solid Waste Combustion Bottom Ash*. *Applied Geochemistry*, 14(1999), pp. 1073-1091. [2]
- Ferraris, B. & Salvo, M. (2001). Glass Matrix Composites from Solid Waste Materials. *Journal of the European Ceramic Society*, 21(2001), pp. 453-460. [3]
- Moir, G. K. & Glasser, F. P. (1974). *Phase Equilibria in the System $\text{Na}_2\text{SiO}_3\text{-CaSiO}_3$* . *Physics & Chemistry of Glasses* 15, pp. 6-11. [4]
- Morey, G. W. (1930). The Devitrification of Soda-Lime-Silica Glasses. *Journal of the American Ceramic Society* 13, pp. 683-713. [5]
- Morey, G. W. & Bowen, N. L. (1925). The Melting Relations of the Soda-Lime-Silica Glasses. *Journal of the Glass Technology Society*, 9, pp. 226. [6]
- Reijnders, L. (2005). *Disposal, Uses & Treatments of Combustion Ashes*. *Resources, Conservation & Recycling*, 43, pp. 313-336. [7]
- Segnit, E. R. (1953). Further Data on the System $\text{Na}_2\text{O-SiO}_2\text{-CaO}$. *American Journal of Science* 251, pp. 586-601. [8]
- Shahid, K. A. & Glasser, F. P. (1971). *Phase Equilibria in the Glass Forming Region of the System $\text{Na}_2\text{O-CaO-SiO}_2$* . *Physics & Chemistry of Glass* 12, pp. 50-57. [9]
- Williamson, J. & Glasser, F. P. (1965). *Phase Relations in the System $\text{Na}_2\text{Si}_2\text{O}_5\text{-SiO}_2$* . *Science* 148, pp. 1589-159. [11]
- Xiao, Y., Oorsprong, M., Yang, Y. & Voncken, J. (2008). *Vitrification of Bottom Ash from a Municipal Solid Waste Incinerator*. *Waste Management*. Vol. 28, pp. 1020-1026. [10]